E214: ATLAS

Bence Mitlasóczki*and Benoît Scholtes†
Rheinische-Friedrich-Wilhelms Universität Bonn

May 2, 2018

Abstract goes here

1 Introduction

Introduction text

2 Theory

Our current best understanding of particle physics is the Standard Model of particle physics (SM). This model describes our discoveries of fundamental particles and their interactions with each other, mediated by fundamental forces. It furthermore describes the way these particles and forces combine to form atoms, from which many of the physical phenomena we encounter in everyday life can be explained. The main shortcoming of the SM however, is its inability to be united with gravity. That said, due to the relative weakness of gravity in comparison to the other fundamental forces, it rarely has an effect in particle physics and thus is mainly ignored (also in this paper).

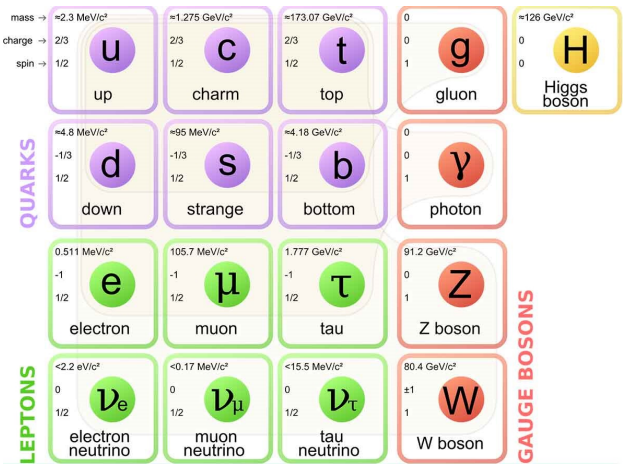

Figure 1: Illustration of the elementary particles in the SM. Quarks are in purple and Leptons in green, arranged into generation columns from left to right. The gauge bosons are in red, with the scalar Higgs boson in yellow.[2]

2.1 The Standard Model

Figure 1 give a summary of the particles in the SM with their most basic properties. Furthermore, there also exists anti-particles of many of these particles. An anti-particle, such as a positron, is identical to its particle (electron) apart from having the opposite electric charge. A neutral particle is often its own anti-particle such as the Z boson, though neutrinos have anti-particles which are merely distinct by having opposing spin projections. All matter particles and the W bosons have anti-particles while the rest are their own anti-particles. Quarks and leptons make up all the matter particles that have been discovered. These are given in three generations of particles, shown with the columns from left to right in the figure. Matter that is encountered everyday is largely structured from the first generation, namely the electron, electron neutrino, up quark, and down quark. For example, atoms are made up of electrons, protons, and neutrons, the latter two being composed of up and down quarks. The second and third generations are composed of particles which are otherwise exactly identical to their first generation counterpart apart from being heavier, the third generation being the heaviest of them all. This is only known to be true for the charged leptons (electron, muon, and tau) and quarks however. Though the neutrinos are known not to be massless, they have very small masses which have not been accurately measured. It is unknown which is the most massive and which the least.[1] Figure 2 illustrates the relative masses of the matter particles. The main reason why the second and third generation of particles are largely not existent in everyday phenomena is due to the requirement that higher energies are needed to produce these heavier particles. Furthermore, these heavier particles have shorter lifetimes due to their favourable decay into lighter particles, such as those in the first generation, due to the fundamental tendency of physical systems to higher kinetic energy states. Particle physics experiments need to be performed at increasingly higher energies in order to produce more massive particles that we do not readily observe. This is illustrated in Figure 3. It should

*s6bemitl@uni-bonn.de
†s6bescho@uni-bonn.de

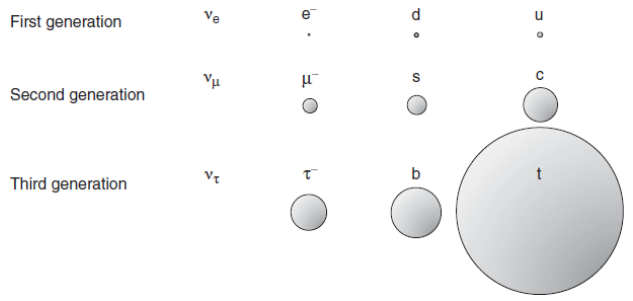

Figure 2: Illustration of the relative masses of the matter particles in their respective generations. The neutrinos are left blank to show that their masses are extremely small in comparison the other particles.[1]

be noted that though neutrinos are not seen, trillions of solar neutrinos pass through your body each second, oscillating between their three different flavours.[1] They are extremely difficult to detect due to the fact that they have a small mass and no electric charge.

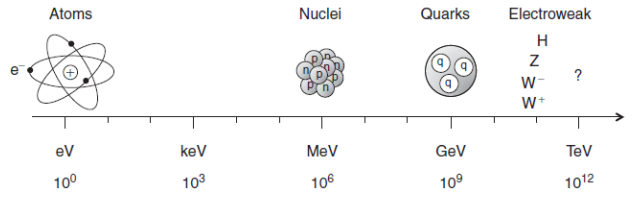

Figure 3: Illustration of the energies required to probe different structures and particles.[1]

Figure 1 also shows the fundamental forces in the SM which are all mediated via the exchange of a gauge boson. The most familiar of these is the photon γ which mediates the electromagnetic force, responsible for electricity, magnetism, and light. The photon interacts with all particles that have an electric charge and thus with all matter particles in the SM apart from the neutrinos. It also interacts with the W bosons as they are electrically charged. The gluon gauge bosons mediate the strong force, thus called as it is the strongest force and binds nuclei and hadrons together, explained in Section 2.2. The gluons interacts only with particles which have a so-called "colour" charge, another property of particles similar to electric charge. Only quarks have a colour charge and the eight differently coloured gluons. Next, the oppositely charged $W^{\pm}$ and Z bosons mediate the weak interaction, the weakest force apart from gravity. This force is responsible for radioactive decay and interacts with all matter particles in the SM. Finally, the Higgs boson is the most recently discovered particle which gives mass to all the matter particles in the SM by interacting with them.

2.2 Hadrons and the Strong Force

Though quarks are elementary in the SM, they cannot be observed as free particles. This is because quantum chromodynamics (QCD) of the SM, the theory of the strong force, states that colour is confined such that systems with a colour charge cannot propagate freely, termed *colour confinement*. Instead, only colourless composite particles can be observed. As a result, quarks form composite particles called hadrons which are bound by gluons. Hadrons generally form baryons, composed of three quarks, and mesons, composed of one quark and one anti-quark. The reason for the these two types is a result of there being three colours, red, blue, and green, for the quarks, and three anti-colours, anti-red, anti-blue, and anti-green, for the anti-quarks. Colourlessness is achieved by combining all three colours (or anti-colours) in a baryon, or a colour and its anti-colour in a meson, as shown in Figure 4. Protons and neutrons are examples of baryons, composed of two up quarks and one down quark (written as uud), and two down quarks and one up quark (udd), respectively. Further-

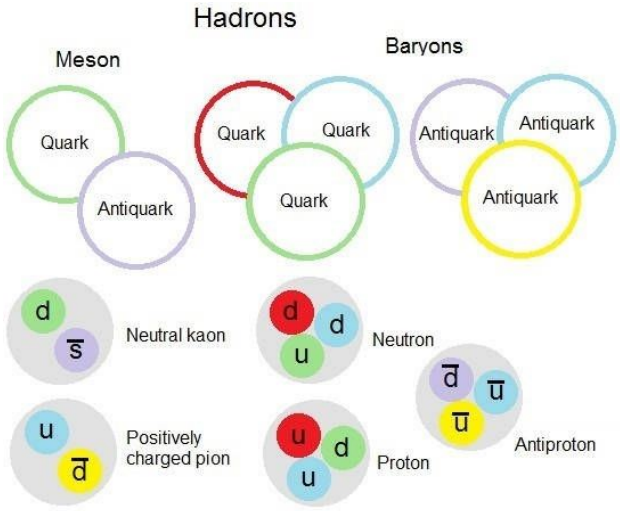

Figure 4: Colour confinement resulting in baryons and mesons, given with some examples.[3]

more, exotic hadrons, which achieve colour confinement with more quarks, have been hypothesised and observed, though without explicit confirmation that the observations were indeed bound exotic hadrons.[1] Examples include the tetraquark with two quarks and two respective anti-quarks, and the pentaquark with four quarks and an anti-quark. Exotic hadrons are rare however, due to the tendency of quarks to form and decay quickly into mesons and baryons.

2.3 The Structure of Protons

The inner workings of hadrons need to be properly considered to accurately model hadronic interactions, ex-

panding on the simplifications of the previous section. Importantly, there does not merely exist three *valence quarks* in baryons, those required to achieve colourlessness. Rather, the binding gluons also split into $q\bar{q}$ pairs, producing extra quarks called *sea quarks*.[5] These gluons and sea quarks then carry part of the baryons momentum and it is these *partons* that interact with other particles. Figure 5 shows this phenomena in a proton-proton interaction. In order to model collisions accurately, such

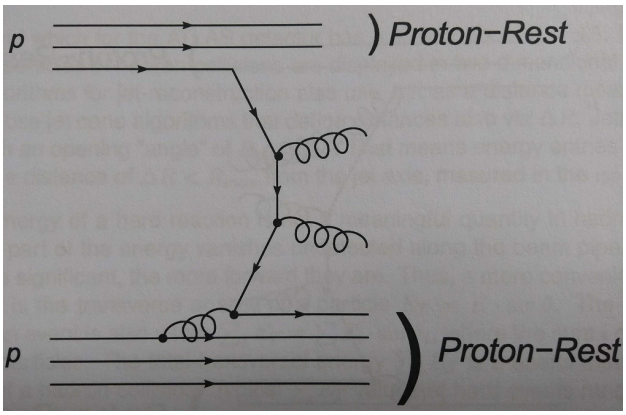

Figure 5: Feynman diagram of proton-proton collision, namely between a valence quark (top) and a sea quark. The two produced gluons here will immediately *hardonise*, form into hadrons, as a result of colour confinement. Thus, this interaction produces two protons and two hadron jets.[5]

as the proton-proton collisions at the LHC, the kinematics of the partons need to be used, derived from parton distribution functions (PDF). These functions describe relative momentum of the different partons as a fraction of the baryon's momentum. They are determined from experiments and depend on the energy scale of the interactions. At the energy scale of the LHC, most proton-proton interactions are of their sea quarks and not valence quarks.[5] One needs to consider all possible reactions however and observe the products of the interaction, such as the number of jets and their momenta, to identify the interaction.

2.4 The Heavy Gauge Bosons[5]

2.4.1 Production, Detection

Apart from the massless photon, there are three massive gauge bosons in the Standard Model, the neutral Z^0 and the charged $W^{\pm}$ bosons.

The Z^0 boson has a mass of 91.1876 ± 0.0021 GeV. The main decay mode is through jets ($\approx 70\%$). For our purposes, the decay to a lepton-antilepton pair (each lepton flavour having a branching ratio of $\approx 3.6 - 3.7\%$) is the important mode, as it is easier to work with lepton tracks than jets because of the amount of QCD background jets.

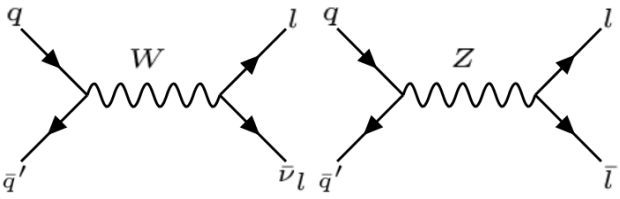

Figure 6: W boson production and decay

The $W^{\pm}$ bosons have a mass known with an order of magnitude higher uncertainty: 80.403 ± 0.029 GeV. They decay to jets with the highest probability ($\approx 68\%$), and the lepton (e, μ)-lepton antineutrino decay modes are looked for in the experiment (the branching ratios are $\approx 10.6 - 11.3\%$ for each flavour). Both the W and Z bosons are produced in the weak Drell-Yan process (see Figure 6) The $Z^0 \to ee/\mu\mu$ processes can be precisely reconstructed from the ATLAS data, although there is a (suppressed) background from QED Drell-Yan pairs. In the case of $W \to e\bar{\nu}_e/\mu\bar{\nu}_\mu$ decays, the neutrino is not detected and needs to be reconstructed from the missing transverse momentum. To a good approximation, both the Z and the W bosons decay at rest, thus the two final state particles have the same momentum, in the opposite direction. We will utilize the precisely known Z^0 mass in Section 4, and consider the case of the W-boson mass below.

2.4.2 The Jacobi Peak[5]

Let us examine the W-boson decay. The final state leptons have an approximate angular distribution

$$\frac{d\sigma}{d\cos\theta^*} = 1 + \cos^2\theta^*,$$

where θ^* denotes the angle between the lepton track and the beam axis. With this knowledge, we can calculate

$$\frac{d\sigma}{dp_T} = \frac{d\sigma}{d\cos\theta^*}\left|\frac{dp_T}{d\cos\theta^*}\right|^{-1} = \frac{d\sigma}{d\cos\theta^*} \cdot \frac{\frac{2p_T}{M_W}}{\sqrt{\left(\frac{M_W}{2}\right)^2 - p_T^2}}$$

This curve clearly has a pole at $p_T = \frac{M_W}{2}$, called the Jacobi peak. There should be no events with $p_T > \frac{M_W}{2}$ in a decay of the W-boson at rest. In reality, there are three distorting effects: first, the detector is made of multiple parts each having a different sensitivity, or even not working, contributing to somewhat imprecise measured (and missing) momenta. Second, the W-boson mass has a Breit-Wigner type distribution centered at M_W. The p_T distribution should reflect this as well. Third, the W-boson at the tree level has no transverse momentum (this assumption is made to derive the formula above), but the radiational corrections allow for some initial p_T. An example process is shown in Figure 7. In the ideal case, one can easily declare the measured mass as the peak in

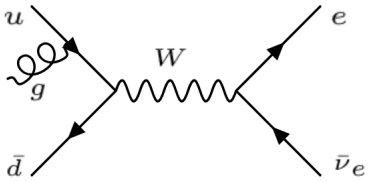

Figure 7: Feynman diagram of a W-boson production with initial state radiation, giving the W-boson transverse momentum.

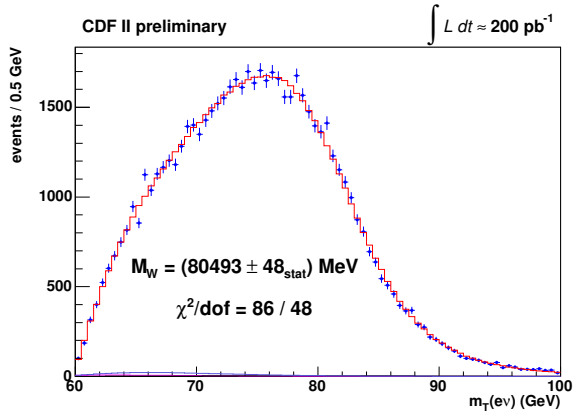

Figure 8: An example of the expected electron transverse momentum histogram.[6]

the histogram, but the smoothening effects make it necessary to employ a ruse. We take advantage of the available simulated data sets with different (known) masses. By fitting a function and extracting the transverse momentum corresponding to the half maximum, we can get a good estimation to what mass the half maximum of the real data fitting corresponds to.

2.5 Extensions to the SM

Though the SM has been extremely successful at describing fundamental physics, it has several shortcomings which necessitate explanations from new physics. Of these, some of the most significant are the inability of the SM to explain neutrino oscillations, gravity, dark matter, and the hierarchy problem. The latter is the observed discrepancy between the strengths of the fundamental forces. The strengths are quantified by coupling constants of the relevant gauge bosons with the relevant charge (gluons with colour charge) and these "constants" actively depend on the energy scale of the interactions. That said, if a grand unified theory (GUT) of the three fundamental forces is to be established, whereby the forces are unified at some higher energy scale, it is expected that the strengths of the different coupling constants converge at this scale, a phenomena which is seemingly not achieved within the SM.

There are numerous theories which attempt to solve the different problems of the SM. One more promising theory is supersymmetry (SuSy) which proposes solutions to the hierarchy problem and provides a candidate dark matter particle. The minimal supersymmetric extension to the SM (MSSM) states that each lepton in the SM has a bosonic superpartner of spin 0, while every boson has a fermionic superpartner of spin 1/2. Figure 9 shows the MSSM particle spectrum. The superparticles

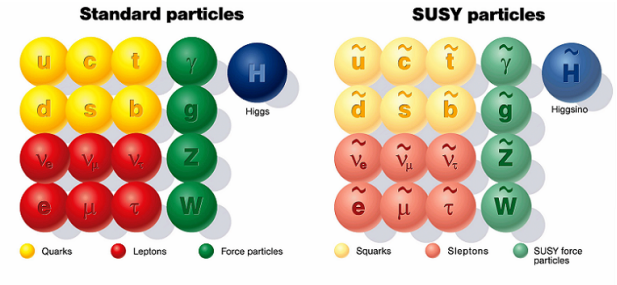

Figure 9: Particles in the MSSM.[7]

have undefined mass, as MSSM particles of mass equal to their superpartners have not been found. As particle physics experiments such as the LHC have not found any MSSM particles yet, it is likely that they have much larger masses not probed yet by the LHC, if MSSM is indeed accurate. MSSM introduces a conserved and multiplicative quantum number called R-parity, defined as $R = (-1)^{3B+L+2S}$, where B is baryon number, L is lepton number, and S is spin. SM particles have +1 R-parity while superparticles have -1 R-parity. As a result, a superparticle cannot decay into SM particles without violating R-parity. Thus, the lightest supersymmetric particle (LSP) must be stable. This is the natural dark matter particle candidate introduced by SuSy. Furthermore, with SuSy the three fundamental force coupling constants do indeed approximately unite at a scale of 10^{16} GeV, solving the hierarchy problem. Searching for evidence of SuSy is currently one of the main goals of the LHC as this would be a major leap in our understanding of physics. As of yet, no such signature have been observed. Other searches of new physics include additional heavy bosons proposed by other SM extension theories, such as bosons similar to the Z boson yet heavier. Furthermore, searches of higher generations of quarks and leptons in the SM are also conducted since they could very well exist yet are so massive that they have not been able to be produced in particle collisions. The LHC can easily investigate such proposals yet is limited in the energy of collisions and thus the masses of the produced particles.

3 The ATLAS Detector

To detect the various particles created by the collisions, the ATLAS detector consists of several layers. Figure 10 is a cross-sectional perspective of the detector.

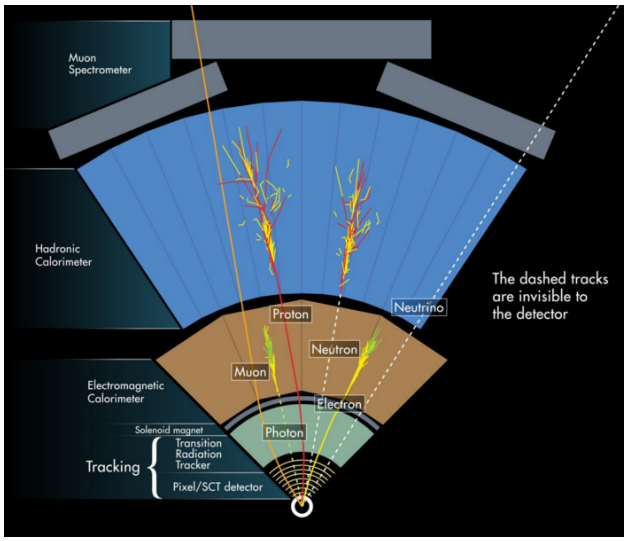

Figure 10: Cross-sectional view of the ATLAS detector showing the different detectors at different layers and how different particles interact with the different detectors. Most of the muon spectrometer is not included in this image.[5]

3.1 Inner Detector

The inner detector helps determining the particle paths as precisely as possible. A solenoid magnet surrounds this system, creating a $\vec{B} = 2$ T magnetic field in which a particle with charge q and velocity $\vec{v}$ experiences a Lorentz force of

$$\vec{F} = \frac{d}{dt}\vec{p} = q\vec{v} \times \vec{B}.$$

From the observed radius of the track of the particle, its momentum and charge sign can be determined allowing for a kinematic analysis of the collision. One can see in Figure 10 how the charged particles are bent by the magnetic field in the inner detector.

- The innermost layer consists of semiconductor pixels (pixel detector, PD), which allow for precise spatial reconstruction of vertices.
- The semi-conductor tracker layer (SCT) serves the same purpose, but with long strips that make covering a larger surface area more practical.
- The transition radiation tracker (TRT) consists of thin, long tubes (drift chambers) with inhomogeneous medium filling in the space between them. A particle passing through this medium emits transition radiation. The photons created this way, along with the particle itself, interact with the gas inside the tubes, causing ionizing. As there is a voltage applied to an electrode in the middle and the tube, the electrons are drawn to the electrode, contributing to an electric pulse. As the transition radiation is strongest for particles with high velocity, the strength of the signal can be used to identify the lightest particles, electrons and positrons.
- The solenoid superconductor magnet mentioned above, creating the magnetic field $\vec{B}$. The magnetic field is parallel to the colliding protons so as not to deflect them before collision.

3.2 Outer Layers

The layers surrounding the inner detector are largely used to determine the energies of the particles. It is composed of three sections.

3.2.1 Electromagnetic Calorimeter

The electromagnetic calorimeter (ECAL) is made of accordion-shaped lead and stainless steel sheets responsible for interacting electromagnetically with the particles passing through, creating an electromagnetic shower, seen in Figure 10. The liquid argon between the lead and steel sheets is ionized by the particles passing through, and the created free electrons are drawn to a copper electrode. An electromagnetic shower is caused by the radiation emitted from bremsstrahlung and compton scattering of the charged particle, whereby the emitted photons then pair-produce, which themselves emit radiation. This cycle continues until photons are emitted which aren't energetic enough to pair-produce. The shower of electron, positron, and photons produced are the electromagnetic shower, which deposits its energy in the detector allowing for a determination of the original particles energy. This calorimeter stops photons, electrons and positrons entirely and single handedly allows for a calculation of their energies. Hadrons and muons also deposit some energy here, but they pass through to reach the outer layers. The cooling system is a cryostat.

3.2.2 Hadron Calorimeter

The hadron calorimeter (HCAL) interacts strongly with the entering particles. The iron tiles induce hadronic showers, identical to the electromagnetic showers but caused hadrons colliding inelastically with the nuclei of the calorimeter material. The particles thus created enter the scintillation tiles producing light, and these photons are carried away in an optical fibre to a unit which measures light intensity, from which the deposited energy can be calculated. The scintillation material is liquid argon, so a cooling system is used in this

layer as well. This calorimeter stops all hardons, leaving only muons and neutrinos to escape this layer of the detector.

3.2.3 Muon Spectrometer

The muon spectrometer is needed to measure the energy of the muons. The muons are so massive that they don't emit bremsstrahlung and don't interact strongly meaning that they only deposit a small amount of their energy in the previous layers of the detector. This unit is supplemented by a larger magnetic system consisting of toroidal magnets such that the detector is capable of determining the momentum of the muons independently of the inner layers. The tiles making up this layer consist of thin tubes filled with gas, and work on the principle of ionization, similarly to the TRT tubes.

4 Procedure

4.1 ATLANTIS

As our first task, we looked at examples of events in the ATLAS detector in the event display software ATLANTIS. This way we got familiar with the working of the ATLAS detector and the signatures of different particles in the detector.

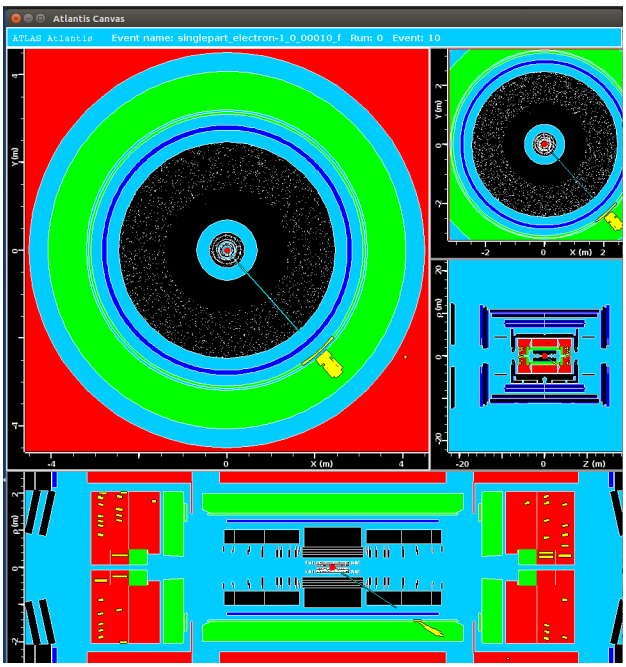

Figure 11: An (artificial) electron track as viewed in ATLANTIS, showing the electromagnetic shower in the ECAL (green).

4.1.1 Electron Energy

We looked at the first 24 electron events in the learning data-set, determining the momentum by the track radius and the energy of the ECAL clusters by manually selecting the region. Figure 11 shows an example of an electron signature in ATLANTIS. The results are summed up in Table 1. The histogram made of the energy/momentum (E/p) ratios is shown in Figure 12. 24 events were chosen as four events were inconclusive as energy was not deposited, leaving 20 meaningful events.

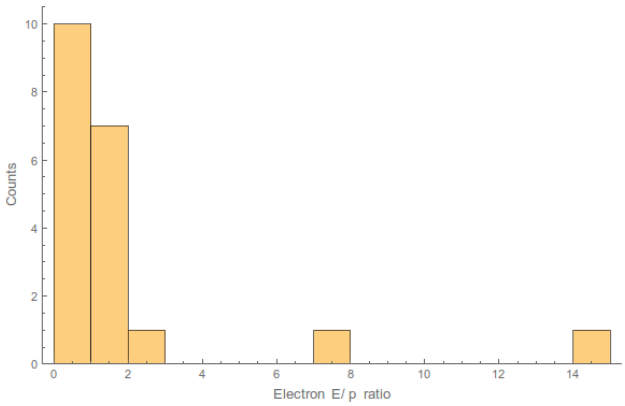

Figure 12: Electron E/p histogram.

From the data, it can be seen that quite a few electrons were measured to have slightly higher momentum than energy, indicating the inaccuracy of the detector. The histogram shows that most electrons were measured with similar energy and momentum, though two relativistic electrons are found with E/p=7.50 and 14.59. A larger sample is required to determine the proper E/p distribution of electrons and whether a higher ratio of relativistic electrons are produced.

4.1.2 Muon Momentum Comparison

As our second task, we compared the measured muon momentum in the muon spectrometer and the inner detector. Calculating the differences between the two methods (Table 2), we noticed some cases where the muon seems to have gained momentum. The average energy loss is 6.87 GeV.

4.2 Electron energy calibration

As the detector is not ideal, we need to calibrate the different regions to account for the differences in their characteristics. We chose sections of $\Delta\eta = 1.25$ and $\Delta\varphi = \pi/2$ ($-2.5 \leq \eta \leq 2.5$, $-\pi < \varphi < \pi$). Using the well-known Z^0 mass, we used cuts to limit ourselves to each of these intervals and iterated the process of scaling the individual values. We also introduced a transverse momentum dependent correction, finally a constant

#	Momentum (GeV)	Energy (GeV)	E/p
1	26.2	54.7	2.09
2	22.78	35.2	1.55
3	244.35	223.2	0.91
4	N/A	N/A	N/A
5	N/A	N/A	N/A
6	66.67	78.3	1.17
7	7.55	56.6	7.50
8	129.82	162.9	1.25
9	3.27	47.7	14.59
10	79.01	66.2	0.84
11	95.93	78.7	0.82
12	37.4	30.6	0.82
13	89.35	86.5	0.97
14	235.24	242.3	1.03
15	105.14	105.3	1.00
16	N/A	N/A	N/A
17	28.62	28.1	0.982
18	53.41	46.4	0.869
19	32.92	64.3	1.95
20	105.64	80.8	0.765
21	N/A	N/A	N/A
22	93.52	82.1	0.878
23	113.98	92.7	0.813
24	155.35	283	1.82

Table 1: The momenta and energies of electrons, determined by the inner detector and ECAL, respectively. The E/p values are subsequently calculated.

shift. Our final *ElecCalib.C* contents can be seen in Section 7. The mass obtained after three iterations is 91.1975 ± 0.0204 GeV, with resolution 2.5315 ± 0.0251, we considered this precise enough for our purposes. Figure 14 shows our fitting.

4.3 Measurement of the W-boson mass

After setting up the electron energy calibration file, we tested it on real ATLAS data, as seen in Figure 15. The mass acquired here is in good agreement with the commonly accepted value. As our next step, we tried scaling the QCD background by comparing the ATLAS data points and our stack-plot. We decided that the scale factor $\alpha = 0.35 \pm 0.05$ gave a fair match (the error was approximated by manual trial). Following the guide, we then set up a macro file to visualize the effect of our cuts on the different data sets of W-boson events with different masses, all at once. The measured half maxima and a linear fitting is shown in Figure 17. We found the linear fitting to be

$$\mathrm{HM}(m) = (0.50267 \pm 0.00867) \cdot m + (2.2613 \pm 0.6898)$$

For the real data, we obtained the half max to be at 43.04 ± 0.09, which gives, after inverting the previous relation, a mass of $m_{\mathrm{W}} = 81.12 \pm 2.03$ GeV.

#	I.D. (GeV)	M.C. (GeV)	Diff. (GeV)	η	ϕ°
1	85.28	53.92	31.36	1.437	21
2	43.4	43.83	-0.43	-0.767	25
3	241.37	237.02	4.350	-2.438	230
4	48.89	44.77	4.12	0.567	311
5	168.16	177.62	-9.46	-1.809	244
6	117.32	96.56	20.76	1.621	152
7	71.94	64.96	6.98	0.699	3.8
8	199.91	199.44	0.470	1.797	67
9	57.84	50.01	7.830	-0.287	241
10	71.1	0	71.1	1.181	312
11	100.75	94.11	6.64	-1.636	48
12	38.26	34.48	3.78	0.189	326
13	105.19	108.68	-3.490	1.163	224
14	236.12	263.61	-27.49	2.286	103
15	131.69	125.51	6.180	-1.763	255
16	152.24	157.69	-5.450	-1.874	27
17	35.23	32.18	3.05	0.395	326
18	54.19	50	4.19	0.229	336
19	84.75	68.09	16.66	0.773	260
20	104.26	107.98	-3.72	1.421	78

Table 2: Muon assignment. The first column shows the Inner Detector measured momentum values, the second column the muon calorimeter momenta, the third column the loss of momentum (negative values show an increase in momentum), the fourth column η, the pseudorapidity, the last column the azimuthal angle.

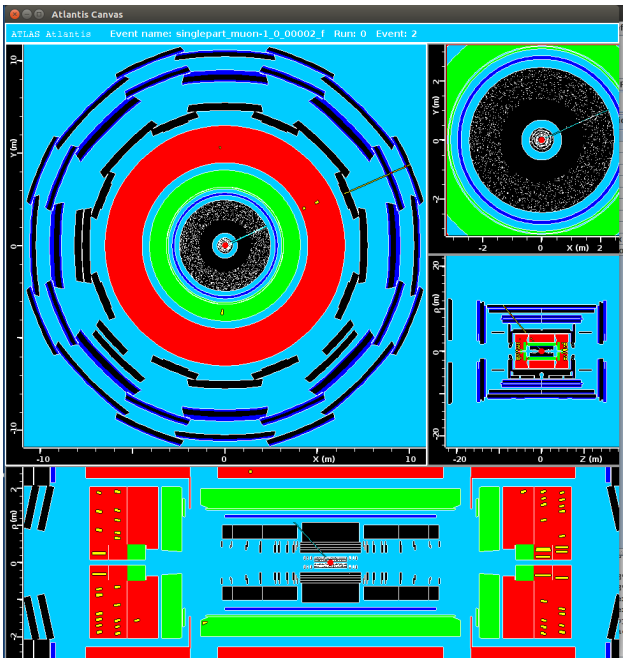

Figure 13: Artificial muon event as seen in ATLANTIS (the panel with quantitive informations has been cropped for better visibility).

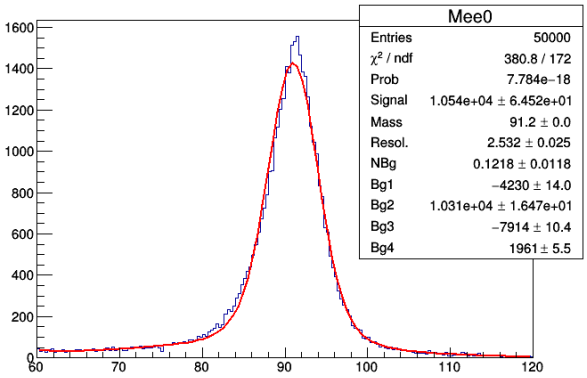

Figure 14: Final iteration fitting of Z^0

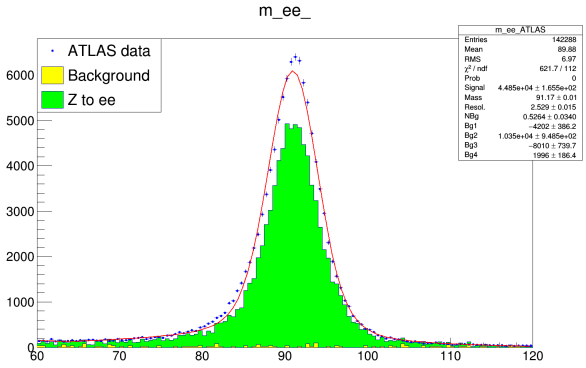

Figure 15: Z^0 mass from ATLAS data

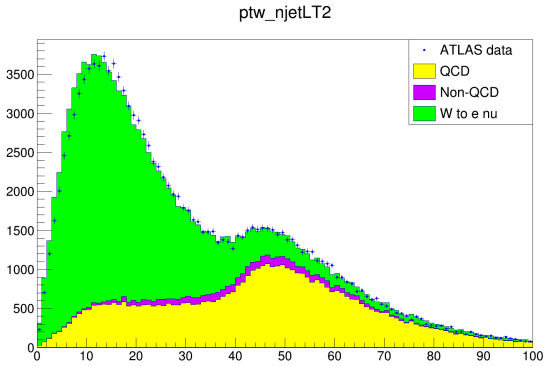

Figure 16: QCD scaled to achieve (by eye) a good match between the stack-plot and the data points.

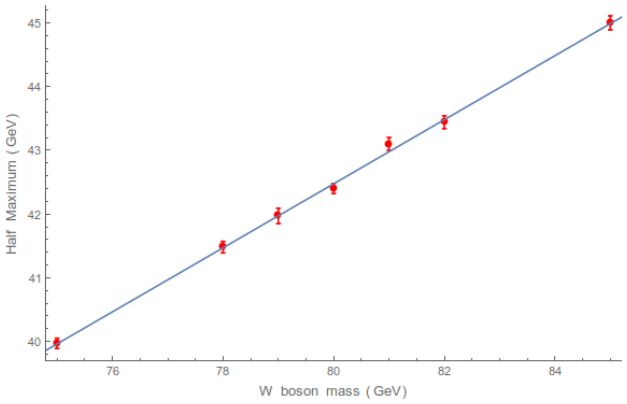

Figure 17: The gauge curve data points with linear fitting.

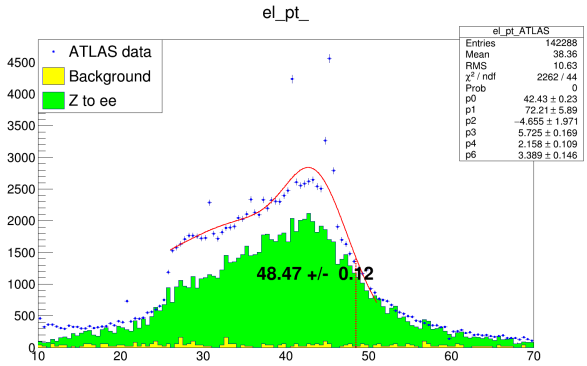

Figure 18: Plot showing the cross-check procedure.

4.4 Cross-check using ATLAS *ee* pair data

The gauge curve can be applied in the case of data for electron-positron pairs. Using the inverse of the gauge function again, we get

$$HM^{-1}(48.47 \pm 0.12) = 91.927 \pm 2.171\,\text{GeV}, \quad (1)$$

in good agreement with the literature value, which supports our previous works.

4.4.1 Error sources

5 Results

6 Conclusion

References

[1] M. Thompson, *Modern Particle Physics* (Cambridge University Press, New York, 2013).

[2] T. DeMichele, *The Standard Model (of Particle Physics) Explained*, WWW

Document, http://factmyth.com/the-standard-model-of-particle-physics-explained/.

[3] H. Klus, *The Strong Nuclear Force*, WWW Document, http://www.thestargarden.co.uk/Strong-nuclear-force.html.

[4] J. Denker, *Quarks ->Mesons ->Nonet = Octet plus Singlet*, WWW Document, https://www.av8n.com/physics/quark-meson-nonet.htm.

[5] Unspecified author, *Advanced Laboratory Course physics601:E214 The ATLAS Experiment* (University of Bonn, 2018).

[6] Hays, C., Kotwal, A., Nodulman, L., Stelzer-Chilton, O., Trischuk, W., Vollrath, I. (2007). *First Measurement of the W Boson Mass with CDF in Run II*.

[7] Unspecified author, *Extensions to the Standard Model?*, WWW Document, http://www.physics.gla.ac.uk/ppt/bsm.htm.

[8] Unspecified author, *Advanced Laboratory Course (physics601): Description of Experiments* (University of Bonn, 2018).

[9] ATLAS Experiment YouTube channel, http://youtube.com/TheATLASExperiment.

[10] W. U. Boeglin, *Scintillation Detectors*, WWW Document, http://wanda.fiu.edu/teaching/courses/Modern_lab_manual/scintillator.html.

[11] Unspecified author, *Gamma Ray Spectroscopy* (University of Florida, 2013), https://www.phys.ufl.edu/courses/phy4803L/group_I/gamma_spec/gamspec.pdf.

[12] E. Ermis and C. Celiktas, International Journal Of Instrumentation Science 1, (2013), pp.54-62.

[13] W. R. Leo, *Techniques for Nuclear and Particle Physics Experiments* (Springer-Verlag, 1987), p. 305.

[14] A. C. Melissinos, J. Napolitano, *Experiments in Modern Physics, 2nd edition* (Academic Press, San Diego, 2003), pp 419-21.

7 Code

```
#include "math.h"
#include "TMath.h"

double ElecCalib(double e_raw, double pt, double eta,
                 double phi, double etiso, double eoverp, double mindrjet)
{
  //double dummy=pt*eta*phi*etiso*eoverp*mindrjet;
  double energy = e_raw ;

if (eta>-2.5 && eta<-2.5/2){
    if (phi> -3.14 && phi< -3.14/2) energy = energy *(91.2/89.79)*(91.19/91.19)*(91.19/91.17);
    else if (phi> -3.14/2 && phi< 0) energy = energy *(91.2/89.76)*(91.19/91.23)*(91.19/91.18);
    else if (phi> 0 && phi< 3.14/2) energy = energy *(91.2/89.69)*(91.19/91.14)*(91.19/91.18);
    else if (phi> 3.14/2 && phi< 3.14) energy = energy *(91.2/89.6)*(91.19/91.09)*(91.19/91.13);
}
else if (eta>-2.5/2 && eta<0){
    if (phi> -3.14 && phi< -3.14/2) energy = energy *(91.2/89.84)*(91.19/91.17)*(91.19/91.15);
    else if (phi> -3.14/2 && phi< 0) energy = energy *(91.2/89.72)*(91.19/91.13)*(91.19/91.17);
    else if (phi> 0 && phi< 3.14/2) energy = energy *(91.2/90.11)*(91.19/91.3)*(91.19/91.25);
    else if (phi> 3.14/2 && phi< 3.14) energy = energy *(91.2/89.92)*(91.19/91.22)*(91.19/91.22);
}
else if (eta>0 && eta<2.5/2){
    if (phi> -3.14 && phi< -3.14/2) energy = energy *(91.2/89.86)*(91.19/91.13)*(91.19/91.16);
    else if (phi> -3.14/2 && phi< 0) energy = energy *(91.2/89.96)*(91.19/91.22)*(91.19/91.22);
    else if (phi> 0 && phi< 3.14/2) energy = energy *(91.2/89.73)*(91.19/91.12)*(91.19/91.16);
    else if (phi> 3.14/2 && phi< 3.14) energy = energy *(91.2/89.91)*(91.19/91.16)*(91.19/91.20);
}
else if (eta>2.5/2 && eta<2.5){
    if (phi> -3.14 && phi< -3.14/2) energy = energy *(91.2/89.92)*(91.19/91.23)*(91.19/91.22);
    else if (phi> -3.14/2 && phi< 0) energy = energy *(91.2/90.01)*(91.19/91.16)*(91.19/91.23);
    else if (phi> 0 && phi< 3.14/2) energy = energy *(91.2/89.82)*(91.19/91.16)*(91.19/91.18);
    else if (phi> 3.14/2 && phi< 3.14) energy = energy *(91.2/89.91)*(91.19/91.12)*(91.19/91.21);
}

if (fabs(pt)>0 && fabs(pt)<20) energy = energy*(91.19/89.26)*(91.19/90.04);
else if (fabs(pt)>20 && fabs(pt)<30) energy = energy*(91.19/90.13)*(91.19/90.79);
else if (fabs(pt)>30 && fabs(pt)<35) energy = energy*(91.19/90.51)*(91.19/90.92);
else if (fabs(pt)>35 && fabs(pt)<40) energy = energy*(91.19/90.68)*(91.19/90.86);
else if (fabs(pt)>40 && fabs(pt)<45) energy = energy*(91.19/91.32)*(91.19/91.1);
else if (fabs(pt)>45 && fabs(pt)<50) energy = energy*(91.19/92.34)*(91.19/91.75);
else if (fabs(pt)>50 && fabs(pt)<60) energy = energy*(91.19/92.31)*(91.19/91.92);
else if (fabs(pt)>60) energy = energy*(91.19/91.89)*(91.19/91.85);

energy = energy - 0.025;


  // if (fabs(eta)>1.5) energy = energy * 91.2/78.2;
  // else if (fabs(eta)>2.0) energy = energy * 91.2/85.4;
return energy;
}
```